Determining the Complex Permittivity of Oil Palm Empty Fruit Bunch Fibre Material by Open-ended Coaxial Probe Technique for Microwave Applications

Daw Mohammad Abdalhadi,[a,*] Zulkifly Abbas,[a,b] Ahmad Fahad Ahmad,[b,*] and Nor Azowa Ibrahim [c]

A material description was established for oil palm empty fruit bunch (OPEFB) fibre waste for microwave absorber applications by determining its dielectric properties with respect to fibre size and frequency. The proposed OPEFB material was studied at frequencies from 1 to 4 GHz. The study was conducted using the open-ended coaxial probe (OECP) HP85071C technique. The effect of microwave frequency on complex permittivity properties for powdered OPEFB and compressed OPEFB with different particle sizes (100, 200, 300, 400, and 500 µm) were investigated. Results showed that the microwave frequency and particle size significantly influenced the complex permittivity (real and imaginary) properties of the samples. Moreover, the complex permittivity decreased as the powder fibre size increased. The complex permittivity of the smallest and largest powder fibre sizes (100 and 500 µm) were (2.050 − *j* 0.197) and (1.934 − *j* 0.137), respectively; and the complex permittivity of the smallest and largest compressed OPEFB fibre sizes (100 and 500 µm) were (3.799 − j0.603) and (3.326 − j0.486), respectively. The compressed OPEFB complex permittivity was higher than that of the OPEFB powder.

Keywords: Oil palm empty fruit bunch; Microwave; Permittivity; Open-ended coaxial

*Contact information: a: Physics Department, Faculty of Science; b: Institute of Advanced Technology; and c: Chemistry Department, Faculty of Science, Universiti Putra Malaysia, 43400 UPM Serdang, Selangor, Malaysia; *Corresponding authors: doibnsahl@gmail.com; ahmad_al67@yahoo. com; ahmadfahad@upm.edu.my*

INTRODUCTION

Material characterization for microwave applications has attracted attention due to huge development of radiofrequency (RF) sources and rapid growth of communication and electronic devices; these have led to an increase of dangerous electromagnetic interference (EMI) issues (Iwamaru *et al.* 2012). In developing microwave applications, identifying a suitable material to meet the requirements is important. Many studies have been focused on the suitability of agricultural waste materials for such applications (Zahid *et al.* 2013), and whether they are fully biodegradable, environmentally friendly, abundantly available, renewable, cheap, and of low density (Yaacoba *et al.* 2015).

Microwave heating is a potential technique for biomass treatment. Therefore, investigating the temperature dependence of the dielectric behavior of the material before exposing it to microwave radiation is imperative. The interaction of the material with microwave radiation depends upon the material dielectric properties (Vassilev *et al.* 2015).

Omar *et al.* (2011) reported that characteristics of empty fruit bunch (EFB) are

comparable to those of other biomass materials. The moisture was found to be sufficiently high to reduce the caloric value, but the high volatility of the material provided high reactivity. The oxygen content was found to be 50%, which gives a low higher heating value (HHV). Moreover, it has been found that the dielectric constant of EFB was proportional to the moisture content, which reaches 60% at 2.45 GHz. The loss factor, however, plateaus above 30% moisture content at frequency below 2 GHz. At the lowest moisture level, *i.e.* 20%, a slight decrease of dielectric constant was observed at lower frequencies. Meanwhile, at above 2 GHz, the dielectric constants for all moisture contents followed the trends of water but at lower values.

Salema *et al.* (2013) and Tripathi *et al.* (2016) studied the effects of microwave frequencies on dielectric properties of oil palm shell (OPS) and oil palm fibre (OPF) using varying frequency in the range 0.2 to 10 GHz. It has been found that the dielectric constant decreased with increasing frequency while the loss factor had a *vice versa* effect against the frequency. Moreover, the temperature dependence of the dielectric properties of OPS and OPS char was reported for the first time. Knowing the temperature dependence of the dielectric properties of a material is important in designing a microwave processing system, because dielectric properties determine the microwave material interaction and whether the dielectric properties change with temperature. Moreover, these properties affect microwave material interactions. The difference in biomass dielectric properties could be attributed to the biomass physical characteristics, moisture content, and material density. The investigation of dielectric properties confirmed the low loss dielectric results of OPS and OPF fibres that were prepared based on the heating characteristics of oil palm biomass under microwave irradiation. On the other hand, biochar is a high microwave absorber and can be used in various microwave applications.

The dielectric properties of semisolid, powdered, or pulverized materials are affected by the composition, including solid particles, air-filled voids that occupy the small spaces between them, as well as material density; whereas permittivity is affected by the wave absorption of the material (Baharudin *et al.* 2013). Moreover, the air constituent that fills up the gap in the spaces between the solid particles of the pulverized material tends to pull down the permittivity values to the permittivity of air. Thus, by removing the air constituent, a permittivity value corresponding to the solid particle is achievable.

Electrical properties, such as volume resistivity and dielectric strength of several natural fibres and composites have been studied (Rana and Singha 2015). For microwave absorbers, material characterization has continued to gather interest due to the vast increase of RF sources and fast growth of electronic devices and communication; this has led to an increase in various EMI issues (Stergiou and Litsardakis 2016; Xie *et al.* 2016). Microwave absorbers can help reduce the signal reflections externally and eliminate unwanted radiation that could interfere with the system operations. Hence, high-performance microwave-absorbing materials with low density, reduced thickness, flexibility, and wide bandwidth are needed (Qin and Brosseau 2012).

A suitable material is needed to improve microwave absorbers to meet these requirements. Recently, researchers have focused on agricultural waste materials (Wei *et al.* 2013). Oil palm empty fruit bunch OPEFB fibres are common in Malaysia, which is considered the largest palm oil exporter worldwide. Malaysia's OPEFB output alone contributes to approximately 19.5 million tons annually (Omar *et al.* 2011). OPEFB is a solid waste product from the oil palm milling process that is extracted from empty fruit

bunches; OPEFB has a high moisture content of approximately 55% to 65% and high silica content of approximately 25%. Therefore, the fibres must be cleaned of oil and dirt (Fahad *et al.* 2015).

OPEFB-reinforcing materials can possibly reduce costs, improve stiffness, enhance thermal stability, and improve the mechanical and dielectric properties of any mixture. Methods for improving the interfacial interaction between fibres and other materials, such as thermoplastics, already exist (Gupta *et al.* 2016). Moreover, studying the dielectric properties of materials has applications in various fields, particularly telecommunications and microwaves (Al-Ghamdi *et al.* 2016).

Several methods can be utilized to determine dielectric properties depending on the material structure (Kundu and Gupta 2014). The coaxial probe technique involves broadband measurement and is used for measuring the complex permittivity of liquids, semi-solids, and powdered materials (Odelstad *et al.* 2014; Jiang *et al.* 2016). The aim of the present study is to present a novel preparation approach for microwave absorbers of compressed substrate and powdered fibre forms. The dielectric properties and complex permittivity of both forms have been investigated using the open-ended coaxial probe (OECP) HP85071C technique at 1 to 4 GHz frequency for different particle sizes (100 to 500 μm). Furthermore, the performance of powdered and compressed forms have been compared.

When an electric field is applied across a dielectric material, three types of impact occur. The first type is surface transmittance, the second type is energy absorbance, and the last type is energy reflection. These impact types help indicate the material electrical properties involved in relative permittivity. Complex permittivity measures the effect of the material on the electric field (Baharudin *et al.* 2013). The mathematical expression of complex permittivity is given by the following equation,

$$\varepsilon^* = \varepsilon' - j\varepsilon'' \quad (1)$$

where ε' is the dielectric constant, or the stored component, and ε'' is the loss factor, or the dissipative component. The loss tangent ($\tan\delta$) is particularly important because it explains the wave absorption of materials, and it is given by the following equation,

$$tan\ \delta = \varepsilon'' / \varepsilon' \quad (2)$$

A greater loss tangent indicates a greater influence of the absorber (Chen 2013).

EXPERIMENTAL

OPEFB Sample Preparation

The OPEFB fibre was obtained from Ulu Langat Oil Palm Mill, Dengkil and Selangor, Malaysia. The samples were prepared in three stages. First, the OPEFB fibres were washed by soaking in distilled water for 24 h to remove the unnecessary wax and other impurities. The fibres were then rinsed with hot water (60 °C) and acetone before oven drying at 80 °C to reduce moisture. In the second stage, a crusher machine (Mainland, Hunan, China) was used to crush the OPEFB fibre chains into powder, which were then sieved through a laboratory test sieve (Endecotts Limited, London, England) to (100, 200, 300, 400, and 500 μm) and sheer each fibre size were placed in a container. Finally, a hot press machine (Yangzhou Hi-tech, Jiangsu, China) was used to prepare a thin sheet (compressed substrate) by placing 20 g (OPEFB) intermixture with polyvinyl

chloride (PVC), which was purchased from Industrial Resin (M) Ltd, to make the sheets easy to compress into rectangular shapes. The powder fibres were pressed with an upper and lower plate temperature of 80 °C for 10 min at a pressure of 110 k/bar. The substrate was left to cool at room temperature. Fig. 1(a, b, c, d) illustrates the OPEFB powder preparation process.

Fig. 1. OPEFB fibre: (a) Dirty fibres, (b) Washed fibres, (c) Crushed fibres, and (d) Compressed fibres

Measurements

Figure 2 illustrates the measurements for the complex permittivity of OPEFB (powder and substrate) using the OECP HP85071C technique (Agilent, Santa Clara, California). The measurement frequency ranged from 1 to 4 GHz at 25 °C room temperature for the 201 frequency points to meet the sample requirement. The probe was connected to the HP 8720B (VNA) Vector Network Analyzer through a high-precision coaxial test cable (Rawat *et al.* 2015).

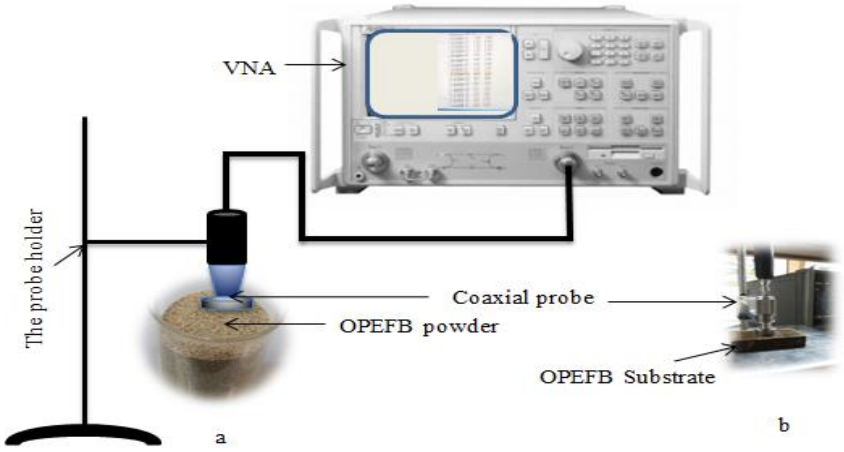

Fig. 2. Complex permittivity measurement procedures: the probe was placed on the material surface of the (a) powder OPEFB fibre, and (b) OPEFB substrate

Figure 3 illustrates the dimensions of the OECP HP85071C that was used in this study. Its outer and inner diameters were $2a$ = 0.66 mm and $2b$ = 3.0 mm, and the diameter of the probe flange was 19.0 mm (Komarov *et al.* 2016). Before the measurement, an inclusive calibration for the complex permittivity measurement was performed using the OPEN (air) SHORT (shorting block) LOAD (distilled water) calibration module to ensure reliable results for complex permittivity for materials under tests.

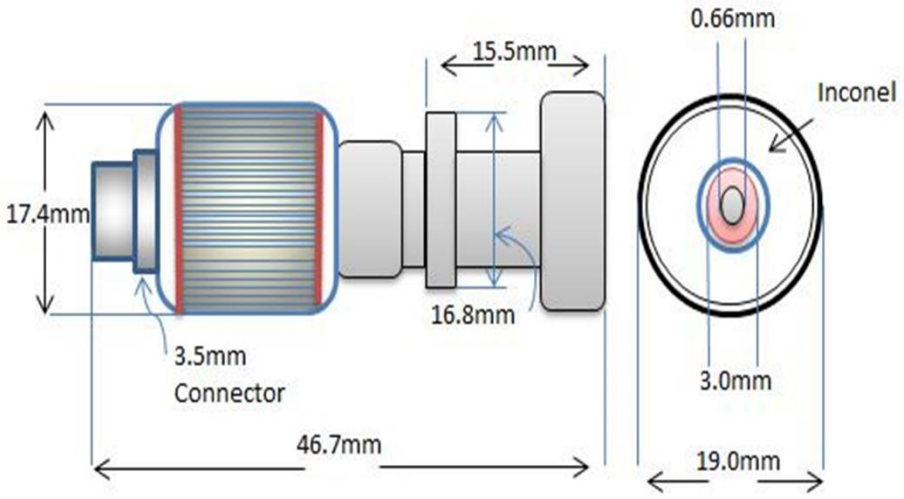

Fig. 3. Schematic diagram of the OECP HP85071C dimensions

Figure 4 illustrates the complex permittivity measurement results for distilled water at 0 to 20 and 1 to 4 GHz at 25 °C, which are recommended for the procedure. Moreover, one can observe that the real part (ε') of permittivity of water is decreasing while the negative imaginary part (ε'') is increasing against frequency. Both the decrease of the real part and the increase of the negative imaginary part do not vary sharply with changes in frequency, and this is due to the relatively small relaxation time.

The measurement results corresponded with literature review results, where the real part began at 78.36 and reached 40.37 at 20 GHz. The imaginary part started from 0.19 and reached 36.56 at 20 GHz. This behavior was due to the dipolar relaxation process, as detected in the liquid-crystalline phase (Francois-Moutal *et al.* 2016).

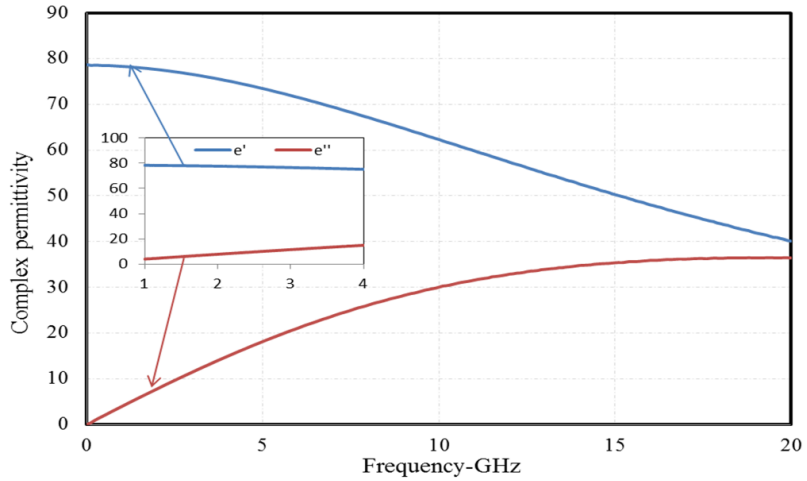

Fig. 4. Complex permittivity of water against frequency

The OECP HP85071C, which measures complex permittivity, was placed on the flat surface of the powder fibres with a width of 60 mm and a height of 55 mm. The fibre thickness in the container was at least 15 mm. This procedure resulted in a field that flowed to the end of the probe, to the fringe, and into the material, finally producing a reflection that can describe the complex permittivity. The measuring equipment came

with an installed software, which made complex permittivity determination easy.

The coaxial probe was placed on the flat surface of the substrate fibres with dimensions (3.5 x 6.1 x 0.8) cm^3. These dimensions were chosen to cover the entire probe circumference and avoid any radiation scattering along the probe edges. For efficient measurement, the manufacturer (Agilent) recommended a minimum thickness of 0.8 cm when using the OECP HP85071C (Teppati *et al.* 2013). Thicknesses below 0.8 cm are prone to uncertainties in dielectric measurement due to the effect of multiple reflections in thin samples. Moreover, the sample must be thick enough and larger than the OECP aperture diameter because this method assumes that the probe does not sense interactions of the electromagnetic field with the sample boundaries.

RESULTS AND DISCUSSION

Complex Permittivity for OPEFB Powder

The electromagnetic wave behavior depends on the dielectric properties ε', ε'', and tanδ. The variations of the dielectric properties of the different-sized OPEFB fibre powders at 100, 200, 300, 400, and 500 μm within a frequency range of 1 to 4 GHz are shown in Fig. 5 (a, b, c). The ε', ε'', and tanδ of the samples decreased at high frequencies. The maximum and minimum values of the ε', ε'', and tanδ within 1 to 4 GHz for all of the samples are listed in Table 1.

The changes in ε', ε'', and tanδ for all samples gradually decreased until the lowest values reached the highest frequency of 4 GHz. Moreover, Fig. 5a shows that the ε' decreased gradually when the frequency increased from 1 to 4 GHz. This decline was caused by the material polarization because of the continuous divergent electric field. This electric field or wave component caused the interaction between the materials and electromagnetic waves (Kappe *et al.* 2012). The reduction of ε' at high frequencies may have been caused by the gradual decrease in the orientation change or dipole movement at high frequencies. Furthermore, the rapid rotation of the dielectric polar molecules was insufficient to attain equilibrium with the field (Raghu *et al.* 2013; Tong 2016).

Investigating the dielectric constant nature as a function of the frequency is important because the dipole may not have enough time to reorganize if the user frequency becomes too high or if it stratifies too fast at lower frequencies. Thus, no heating may occur under these conditions (Kappe *et al.* 2012). In contrast, the wavelength change may clarify the ε' behavior. The dielectric constant changes may have been caused by different physical properties, such as particle size and fibre density. In the OPEFB fibres, a high ε'' caused high absorption loss; thus, the unbending absorptive material was formed using the lowest OPEFB fibre size. Figure 5b shows a similar variation of the ε''. The loss factor for all the fibre sizes had the highest values at the lowest frequencies and smallest fibre size; moreover, these decreased gradually until the lowest loss factors were obtained at 4 GHz and largest fibre size, as shown in Table 1. This switchback-shaped line for the ε'' is visible in all fibre sizes but at various frequency ranges.

Moreover, the tanδ of the OPEFB depended broadly on the ε''. The tanδ value is the tangent of the angle (δ) between the capacity vectors of the total and charging currents (Gregory *et al.* 2016). Figure 5c illustrates the tanδ results calculated using Eq. 2. The tanδ of all the composites indicated that the same ordered behavior of the fibre sizes was due to the increased frequencies and fibre particle rearrangement. The highest

tanδ was obtained at the lowest frequency values and smallest fibre size, as shown in Table 1.

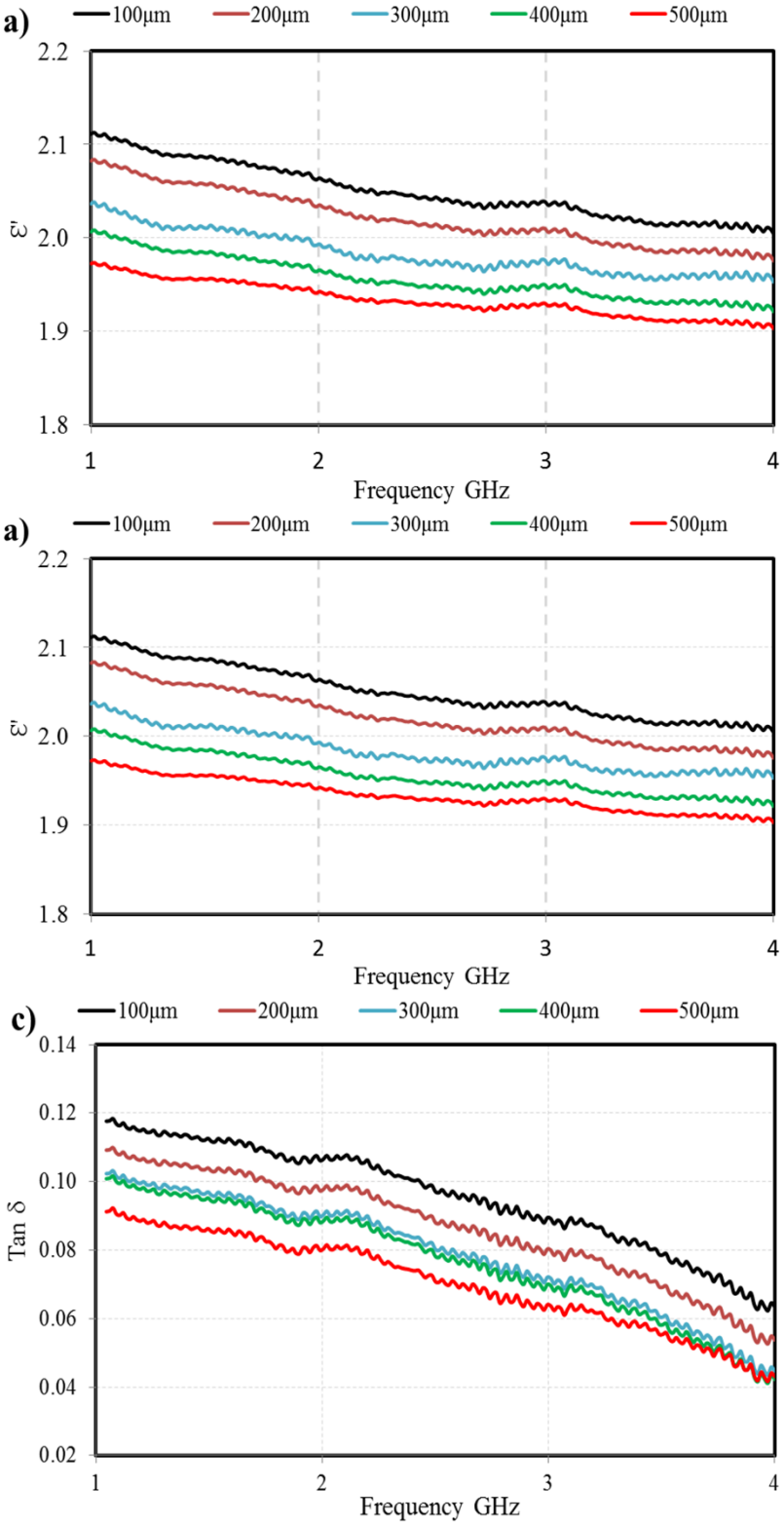

Fig. 5. Variations: (a) Dielectric constant (ε'), (b) loss factor (ε''), and (c) loss tangent (tanδ) against frequency at different OPEFB powder particle sizes

Table 1. Variations in ε', ε'', and Tanδ at 1 and 4 GHz for Different OPEFB Powder Particle Sizes

Fibre Size (μm)	ε'		ε''		tanδ	
	1 GHz	4 GHz	1 GHz	4 GHz	1 GHz	4 GHz
100	2.111	2.004	0.246	0.127	0.117	0.063
200	2.082	1.975	0.225	0.106	0.108	0.054
300	2.037	1.953	0.206	0.087	0.101	0.045
400	2.007	1.921	0.200	0.081	0.100	0.042
500	1.972	1.903	0.182	0.082	0.092	0.043

Table 1 shows that the increased OPEFB fibre size resulted in a decrease of the ε', ε'', and tanδ of the fibre powder. Furthermore, 2.45 GHz is applied in industrial and domestic microwaves (Singh *et al.* 2015). The dielectric properties for OPEFB powder at 2.45 GHz are shown in Table 2. These are evident in Table 2, wherein the results of the ε', ε'', and tan δ for all fibre sizes had the highest values of ε', ε'', and tan δ at the smallest fibre size, and vice versa.

Table 2. Variations of ε', ε'', and Tanδ at 2.45 GHz Frequency for Different Particle Size of OPEFB Powder

Fibre Size (μm)	ε'	ε''	tanδ
100	2.043	0.201	0.098
200	2.014	0.180	0.089
300	1.974	0.161	0.081
400	1.948	0.155	0.079
500	1.929	0.139	0.072

The mean complex permittivity of different OPEFB powder particle sizes was calculated using Eq. 1. Complex permittivity, at frequencies from 1 to 4 GHz, decreased with increased fibre size. This conclusion is clarified and summarized in Table 3.

Table 3. Mean Complex Permittivity of Different OPEFB Powder Particle Sizes at 1 to 4 GHz

Fibre Size (μm)	Relative Permittivity
100	2.050 - *j* 0.197
200	2.021 - *j* 0.176
300	1.983 - *j* 0.157
400	1.956 - *j* 0.151
500	1.934 - *j* 0.137

The variations in the ε', ε'', and tan δ for different fibre sizes and several selected frequencies (1, 2, 3, and 4 GHz) are shown in Fig. 6 (a, b, c). The dielectric properties ε', ε'', and tanδ decreased linearly as the OPEFB fibre size increased for all frequencies.

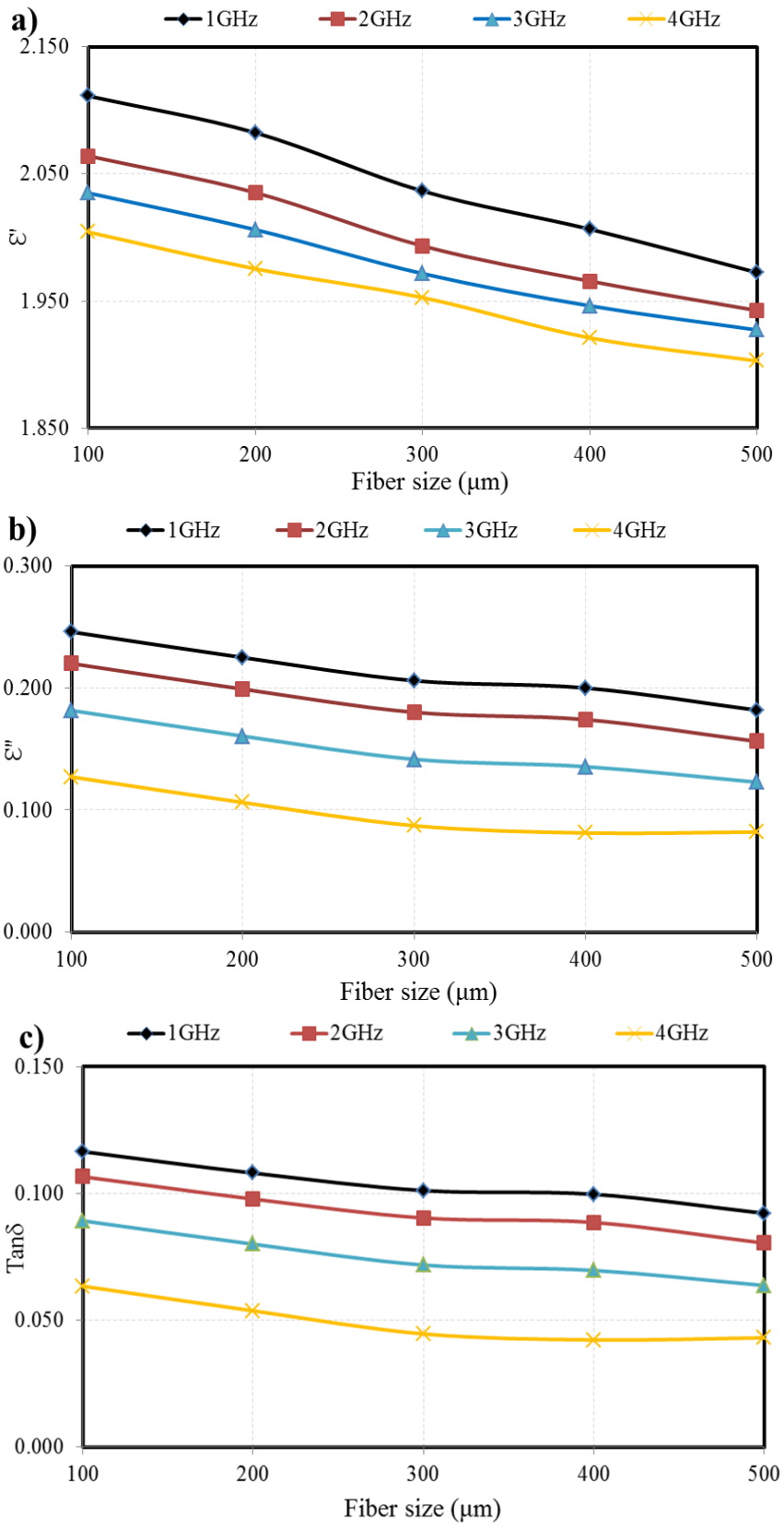

Fig. 6. Variations: (a) Dielectric constant (*ε*'), (b) loss factor (*ε*"), and (c) loss tangent (tan*δ*) against OPEFB powder particle sizes at different frequencies

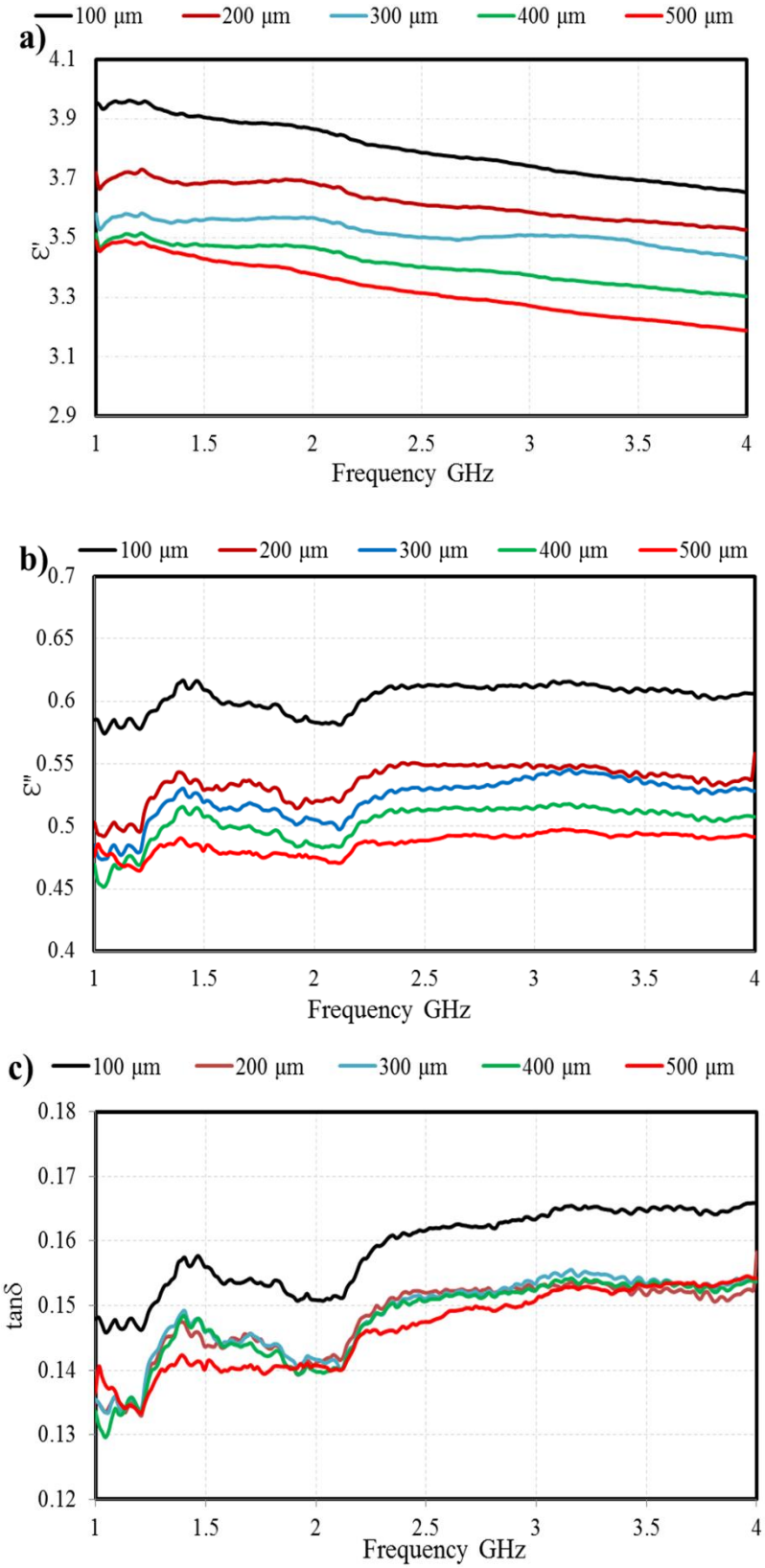

Fig. 7. Variations: (a) dielectric constant (*ε'*), loss factor (*ε''*), and (c) tan*δ* against frequency at different particle sizes of OPEFB powder in substrate form

Complex Permittivity of the Substrate OPEFB at Different Particle Sizes

The dielectric properties at room temperature were measured using the OECP HP85071C technique in the frequency range of 1 to 4 GHz, and the results are presented in Fig. 7 (a, b, c). The compressed substrate of the OPEFB fibre was placed under the probe without a gap to avoid influencing the dielectric value readings.

Figure 7a shows that the dielectric constant values decreased with as fibre substrate frequencies increased; this is more apparent at lower frequencies. The polarizability of the molecules relied on the dielectric constant of the material. A decrease in the orientation polarization at high frequencies caused a decline in the dielectric constant that corresponded to the frequency. At low frequencies, reorientation of the whole direction of the molecule was possible, whereas at medium frequencies, only a small period of time was allotted for orientation. The molecular orientation was impossible at high frequencies.

The changing behaviors of the ε'' and tanδ for all samples were similar. Seemingly, the tanδ of the OPEFB fibres largely depended on ε' and ε''. The loss factor for all of the samples was observed to increase at high frequencies until 1.45 GHz, but it decreased as the frequency increased from 1.45 to 2.25 GHz. After that, the loss factor increased until 4 GHz. These behaviors of loss factor and tangent were seen in all fibre sizes but at different frequencies. The highest and lowest values of the ε', ε'', and tanδ at 1 to 4 GHz are listed in Table 4 for all of the OPEFB fibre sizes in substrate form.

Table 4. Variations of the (ε'), (ε''), and Tanδ for all Particles Size of OPEFB Fibre in Compressed Substrate Form

Fibre Size(μm)	ε'		ε''		tanδ	
	1 GHz	4 GHz	1 GHz	4 GHz	1 GHz	4 GHz
100	3.933	3.643	0.565	0.606	0.148	0.166
200	3.715	3.517	0.503	0.558	0.135	0.158
300	3.585	3.411	0.485	0.528	0.135	0.158
400	3.497	3.296	0.469	0.507	0.134	0.154
500	3.455	3.175	0.456	0.491	0.136	0.154

Universally, industrial and domestic heating applications use the 2.45 GHz microwave frequency. Hence, in Table 5, the dielectric properties of all particle sizes of OPEFB in substrate form use this frequency. Moreover, this is evident in Table 6, where the results of the ε', ε'', and tan δ for all fibre sizes showed the highest values at the smallest fibre size, and *vice versa*.

Table 5. Variations of the (ε'), (ε''), and Tanδ for all Particles Size of OPEFB Fibre in Compressed Form at 2.45 GHz

Fibre Size (μm)	ε'	ε''	tanδ
100	0.612	3.793	0.161
200	0.551	3.616	0.152
300	0.531	3.504	0.152
400	0.513	3.406	0.151
500	0.488	3.318	0.147

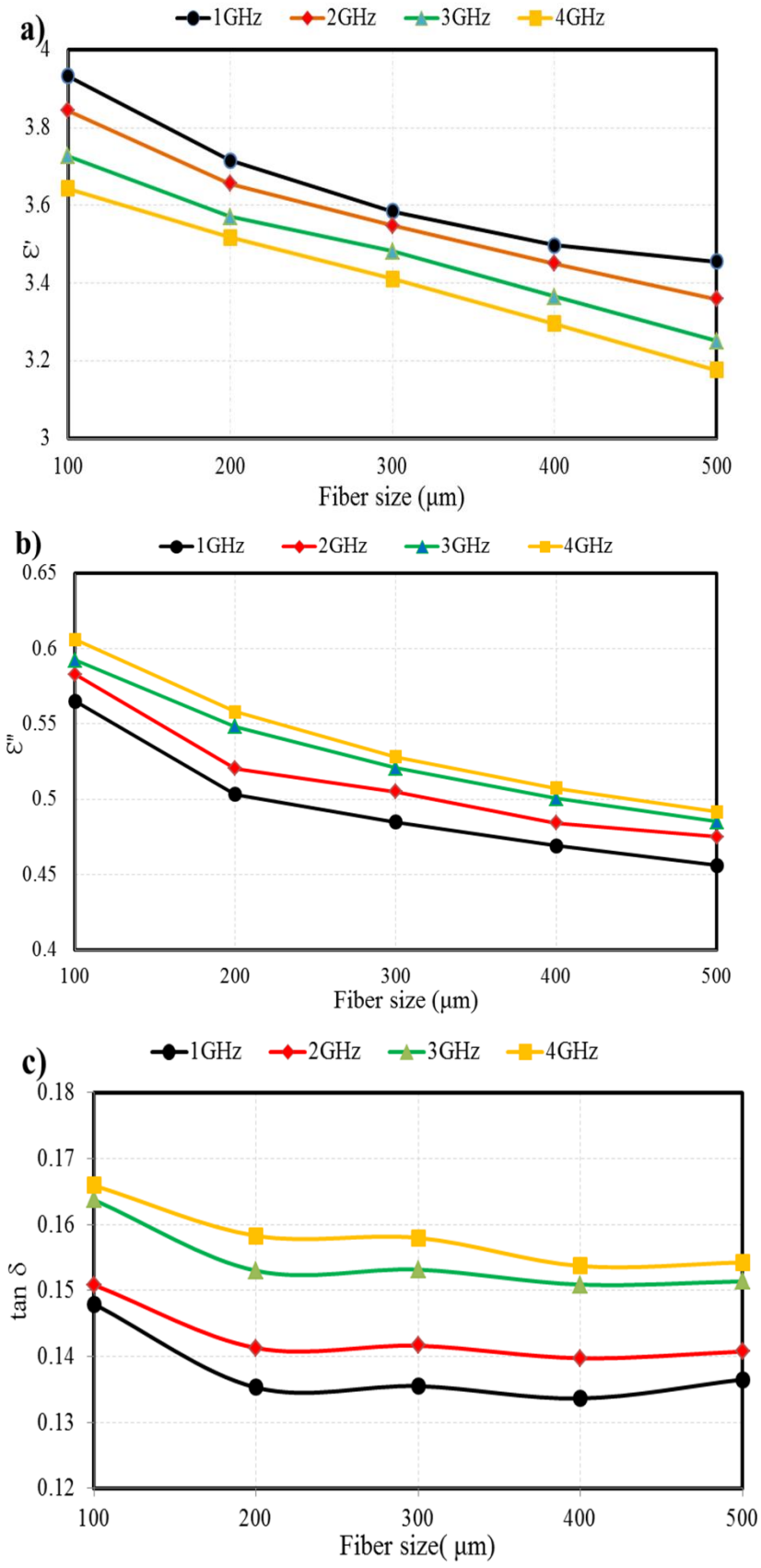

Fig. 8. Variations: (a) Dielectric constant (*ε*'), (b) loss factor (*ε*''), and (c) loss tangent (tan*δ*) against fibre sizes in substrate form

In general, the increased OPEFB fibre size caused a decrease in all dielectric properties of the substrates. In contrast, the ε' for all samples decreased with higher frequencies; moreover, the ε'' and tanδ for all samples increased with higher frequencies. Thus, the average complex permittivity for OPEFB substrate could be calculated using Eq. 1. The mean values of complex permittivity for all fibre sizes at 1 to 4 GHz are summarized in Table 6.

Table 6. Mean Complex Permittivity for all Particle Sizes of OPEFB in Substrate Form at 1 to 4 GHz

Fibre Size (μm)	Relative Permittivity
100	3.799 - *j*0.603
200	3.623 - *j*0.536
300	3.519 - *j*0.523
400	3.409 - *j*0.503
500	3.326 - *j*0.486

To study the effects of substrate fibre size on the dielectric properties, Figs. 8 (a, b, c) show the variations of ε', ε'', and tanδ with fibre size at certain frequencies (1, 2, 3, and 4 GHz) at room temperature. The ε', ε'', and tanδ decreased as fibre size increased due to the moisture absorption at the fibre interface. Notably, as frequency increased, the dielectric constant decreased, which is expected OPEFB behavior (Hu *et al.* 2013). Moreover, the effective dielectric constant possibly decreased with as fibre size increased due to the increased interface volume when a smaller fibre was used for a given volume fraction of filler. At a given volume fraction of fibre, a smaller particle size will have higher interfacial polarization (Suresh *et al.* 2013).

CONCLUSIONS

1. The open-ended coaxial probe OECP HP85071C technique is simple and appropriate for determining the complex permittivity of OPEFB fibres using the magnitude of the reflection coefficient and phase measurement.
2. The powder experiments showed that the highest complex permittivity for the smallest fibres was 2.050 - j 0.197 at 1 to 4 GHz, and the lowest complex permittivity for the largest fibres was 1.934 - j 0.137 at 1 to 4 GHz.
3. The experimental results for the compressed substrate showed that the smallest fibres in compressed form had the highest complex permittivity values 3.799 - j0.603 at 1 to 4 GHz; and the results showed that the lowest complex permittivity was found with the largest fibres particle size, at a value of 3.326 - j0.486 at 1 to 4 GHz.
4. The results showed that the complex permittivity decreased as fibre size and frequency increased due to the orientation polarization and high movement of the polar molecular dipoles.

5. The complex permittivity values of the fibre substrate are larger than those of fibre powders due to homogeneity, particle adhesion, and minimal space between the particles, which led to reduction of air molecules between fibres.

REFERENCES CITED

Al-Ghamdi, A. A., Al-Hartomy, O. A., Al-Solamy, F. R., Dishovsky, N., Mihaylov, M., Malinova, P., and Atanasov, N. (2016). "Dielectric and microwave properties of elastomer composites loaded with carbon–silica hybrid fillers," *J. Appl. Polym. Sci.* 133(7). DOI: 10.1002/app.42978

Alam, A. M., Mina, M. F., Beg, M. D. H., Mamun, A. A., Bledzki, A. K., and Shubhra, Q. T. H. (2014). "Thermo-mechanical and morphological properties of short natural fibre reinforced poly (lactic acid) biocomposite: Effect of fibre treatment," *Fibres and Polymers* 15(6), 1303-1309. DOI: 10.1007/s12221-014-1303-8

Baharudin, E., Ismail, A., Alhawari, A. R. H., Zainudin, E. S., Majid, D. L., Seman, F. C., and Khamis, N. H. (2013). "Determination of pulverized material permittivity for microwave absorber application," in: *Micro and Nanoelectronics (RSM)*, Langkawi, Malaysia, pp. 85-88. DOI: 10.1109/RSM.2013.6706479.

Chen, W. K. (2013). *Theory and Design of Broadband Matching Networks: Applied Electricity and Electronics*, Elsevier. Amsterdam, Netherlands.

Fahad, A., Abbas, Z., Zainuddin, M. F., Jabbar, S., and Yakubu, A. B. (2015). "Dielectric characterization of oil palm fibre reinforced polycaprolactone-nickel oxide composite at microwave frequency," *Procedia Environmental Sciences* 30, 273-278. DOI: 10.1016/j.proenv.2015.10.049

Francois-Moutal, L., Ouberai, M. M., Maniti, O., Welland, M. E., Strzelecka-Kiliszek, A., Wos, M., Pikula, S., Bandorowicz-Pikula, J., Marcillat, O., and Granjon, T. (2016). "Two-step membrane binding of NDPK-B induces membrane fluidity decrease and changes in lipid lateral organization and protein cluster formation," *Langmuir* 32(48), 12923-12933. DOI: 10.1021/acs. langmuir.6b03789

Gregory, A. P., Blackburn, J. F., Lees, K., Clarke, R. N., Hodgetts, T. E., Hanham, S. M., and Klein, N. (2016). "Measurement of the permittivity and loss of high-loss materials using a near-field scanning microwave microscope," *Ultramicroscopy* 161, 137-145. DOI: 10.1016/j.ultramic.2015.11.015

Gupta, A. K., Biswal, M., Mohanty, S., and Nayak, S. K. (2016). "Eco-friendly lignocellulosic natural fibre reinforced recycled polymer composite with modified interface and reactive compatibilization: A micromechanical analysis with various model," *Materials Focus* 5(2), 106-118. DOI: 10.1166/mat.2016.1302

Hu, W., Liu, Y., Withers, R. L., Frankcombe, T. J., Norén, L., Snashall, A., Kitchin, M., Smith, P., Gong, B., Chen, H., *et al.* (2013). "Electron-pinned defect-dipoles for high-performance colossal permittivity materials," *Nature Materials* 12(9), 821-826. DOI: 10.1038/nmat3691

Iwamaru, T., Katsumata, H., Uekusa, S., Ooyagi, H., Ishimura, T., and Miyakoshi, T. (2012). "Development of microwave absorbing materials prepared from a polymer binder including Japanese lacquer and epoxy resin," *Physics Procedia* 23, 69-72. DOI: 10.1016/j.phpro. 2012. 01.018

Jayamani, E., Hamdan, S., Rahman, M. R., and Bakri, M. K. B. (2014). "Comparative study of dielectric properties of hybrid natural fibre composites," *Procedia Engineering* 97, 536-544. DOI: 10.1016/j.proeng.2014.12.280

Jiang, N. N., Yang, Y., Zhang, Y. X., Zhou, J. P., Liu, P., and Deng, C. Y. (2016). "Influence of zinc concentration on structure, complex permittivity and permeability of Ni–Zn ferrites at high frequency," *Journal of Magnetism and Magnetic Materials* 401, 370-377. DOI: 10.1016/j.jmmm.2015.10.003

Kappe, C. O., Stadler, A., and Dallinger, D. (2012). *Microwaves in Organic and Medicinal Chemistry*, John Wiley & Sons, Hoboken, NJ.

Komarov, S. A., Komarov, A. S., Barber, D. G., Lemes, M. J., and Rysgaard, S. (2016). "Open-ended coaxial probe technique for dielectric spectroscopy of artificially grown sea ice," *IEEE Transactions on Geoscience and Remote Sensing* 54(8), 4941-4951. DOI: 10.1109/TGRS.2016.2553110

Kundu, A., and Gupta, B. (2014). "Broadband dielectric properties measurement of some vegetables and fruits using open-ended coaxial probe technique," in: *Control Instrumentation, Energy and Communication (CIEC)*, International Conference on IEEE, pp. 480-484. DOI: 10.1109/CIEC.2014.6959135

Mubarak, N. M., Sahu, J. N., Abdullah, E. C., and Jayakumar, N. S. (2016). "Palm oil empty fruit bunch based magnetic biochar composite comparison for synthesis by microwave-assisted and conventional heating," *Journal of Analytical and Applied Pyrolysis* 120, 521-528. DOI: 10.1016/j.jaap.2016.06.026

Omar, R., Idris, A., Yunus, R., Khalid, K., and Isma, M. A. (2011). "Characterization of empty fruit bunch for microwave-assisted pyrolysis," *Fuel* 90(4), 1536-1544. DOI: 10.1016/j.fuel.2011.01.023

Qin, F., and Brosseau, C. (2012). "A review and analysis of microwave absorption in polymer composites filled with carbonaceous particles," *J. Appl. Phys.* 111(6). DOI: 10.1063/1.3688435

Odelstad, E., Raman, S., Rydberg, A., and Augustine, R. (2014). "Experimental procedure for determination of the dielectric properties of biological samples in the 2-50 GHz range," *IEEE Journal of Translational Engineering in Health and Medicine* 2, 1-8. DOI: 10.1109/JTEHM.2014.2340412

Raghu, S., Kilarkaje, S., Sanjeev, G., and Devendrappa, H. (2013). "Electron beam induced modifications in conductivity and dielectric property of polymer electrolyte film," *Radiation Measurements* 53, 56-64. DOI: 10.1016/j.radmeas.2013.03.017

Rana, A. K., and Singha, A. S. (2015). "Dielectric, flammability and physicochemical properties of surface functionalized *Cannabis indica* fibres reinforced composite materials," *Polymer Science Series A* 57(2), 221-232. DOI: 10.1134/S0965545X15 020145

Rawat, V., Nadkarni, V., Kale, S. N., Hingane, S., Wani, S., and Rajguru, C. (2015). "Calibration and optimization of a metamaterial sensor for hybrid fuel detection," in: *Physics and Technology of Sensors (ISPTS),* 2nd International Symposium on IEEE, pp. 257-259. DOI: 10.1109/ISPTS.2015.7220124

Salema, A. A., Yeow, Y. K., Ishaque, K., Ani, F. N., Afzal, M. T., and Hassan, A. (2013). "Dielectric properties and microwave heating of oil palm biomass and biochar," *Industrial Crops and Products* 50, 366-374. DOI: 10.1016/j.indcrop.2013.08.007

Stergiou, C. A., and Litsardakis, G. (2016). "Y-type hexagonal ferrites for microwave absorber and antenna applications," *J. Magn. Magn. Mater*. 405, 54-61. DOI: 10.1016/j.jmmm.2015.12.027

Suresh, S., Mortensen, A., and Needleman, A. (2013). *Fundamentals of Metal-Matrix Composites*, Elsevier, Amsterdam, Netherlands.

Singha, A. S., Rana, A. K., and Jarial, R. K. (2013). "Mechanical, dielectric and thermal properties of *Grewia optiva* fibres reinforced unsaturated polyester matrix based composites," *Materials & Design* 51, 924-934. DOI: 10.1016/j.matdes.2013.04.035

Singh, S., Gupta, D., Jain, V., and Sharma, A. K. (2015). "Microwave processing of materials and applications in manufacturing industries: A review," *Materials and Manufacturing Processes* 30(1), 1-29. DOI: 10.1080/10426914.2014.952028

Tong, X. C. (2016). *Advanced Materials and Design for Electromagnetic Interference Shielding*, CRC Press, Boca Raton, Florida.

Teppati, V., Ferrero, A., and Sayed, M. (eds.). (2013). *Modern RF and Microwave Measurement Techniques*, Cambridge University Press.

Vassilev, S. V., Vassileva, C. G., and Vassilev, V. S. (2015). "Advantages and disadvantages of composition and properties of biomass in comparison with coal: An overview," *Fuel* 158, 330-350. DOI: 10.1016/j.fuel.2015.05.050

Wei, L., Che, R., Jiang, Y., and Yu, B. (2013). "Study on preparation and microwave absorption property of the core-nanoshell composite materials doped with La," *J. Environ. Sci.* 25(S1), S27-S31. DOI: 10.1016/S1001-0742(14)60620-3

Xie, W., Zhu, X., Yi, S., Kuang, J., Cheng, H., Tang, W., and Deng, Y. (2016). "Electromagnetic absorption properties of natural microcrystalline graphite," *Mater. Design* 90, 38-46. DOI: 10.1016/j.matdes.2015.10.115

Yaacoba, W., Nadiah, W. S., Jamarib, S. S., and Ghazalic, S. (2015). "Effect of particle size of natural based carbon filler to the absorbency of superabsorbent polymer composite synthesis by graft polymerization method," in: *Advanced Materials Research* 1119, 301-305. DOI: 10.4028/ /AMR.1119.301.

Zahid, L., Malek, M. F. B. A., Nornikman, H., Mohd Affendi, N. A., Ali, A., Hussin, N., Ahmad, B. H., and Abdul Aziz, M. Z. A. (2013). "Development of pyramidal microwave absorber using sugarcane bagasse (SCB)," *Progress in Electromagnetics Research* 137, 687-702. DOI:10.2528/PIER13012602.

Article submitted: November 9, 2016; Peer review completed: January 7, 2017; Revised version received: February 26, 2017; Second revision received and accepted: March 13, 2017; Published: April 14, 2017.
DOI: 10.15376/biores.12.2.3976-3991